Understanding ENSO diversity

By Antonietta Capotondi, Andrew T. Wittenberg, Matthew Newman, Emanuele Di Lorenzo, Jin-Yi Yu, Pascale Braconnot, Julia Cole, Boris Dewitte, Benjamin Giese, Eric Guilyardi, Fei-Fei Jin, Kristopher Karnauskas, Benjamin Kirtman, Tong Lee, Niklas Schneider, Yan Xue, Sang-Wook Yeh

Antonietta Capotondi - University of Colorado and NOAA Earth System Research Laboratory, Boulder, Colorado
Andrew T. Wittenberg – NOAA Geophysical Fluid Dynamics Laboratory, Princeton, New Jersey
Matthew Newman - University of Colorado and NOAA Earth System Research Laboratory, Boulder, Colorado
Emanuele Di Lorenzo - Georgia Institute of Technology, Atlanta, Georgia
Jin-Yi Yu - University of California, Irvine, California
Pascale Braconnot – Laboratoire des Sciences du Climat et de l'Environnement, Gif-sur-Yvette, France
Julia Cole – University of Arizona, Tucson , Arizona
Boris Dewitte – LEGOS, Toulouse, France
Benjamin Giese - Texas A&M, College Station, Texas
Eric Guilyardi – LOCEAN/IPSL, Paris, France, and University of Reading, Reading United Kingdom
Fei-Fei Jin – University of Hawaii, Honolulu, Hawaii
Kristopher B. Karnauskas – Woods Hole Oceanographic Institution, Woods Hole, Massachusetts
Benjamin Kirtman – University of Miami, Miami, Florida
Tong Lee – Jet Propulsion Laboratory, Pasadena, California
Niklas Schneider – University of Hawaii, Honolulu, Hawaii
Yan Xue – Climate Prediction Center, College Park, Maryland
Sang-Wook Yeh – Hanyang University, Ansan, South Korea

Corresponding author address: Antonietta Capotondi, NOAA/ESRL/PSD1, 325 Broadway, Boulder, CO, 80305. Email: Antonietta.Capotondi@noaa.gov

Capsule

Improved determination of ENSO predictability, teleconnections and impacts requires a better understanding of event-to-event differences in ENSO spatial patterns and evolution.

Abstract

The El Niño Southern Oscillation (ENSO) is a naturally occurring mode of tropical Pacific variability, with global impacts on society and natural ecosystems. While it has long been known that El Niño events display a diverse range of amplitudes, triggers, spatial patterns, and life cycles, the realization that ENSO's impacts can be highly sensitive to this event-to-event diversity is driving a renewed interest in the subject. This paper surveys our current state of knowledge of ENSO diversity, identifies key gaps in understanding, and outlines some promising future research directions.

Introduction

The El Niño Southern Oscillation (ENSO) is a naturally occurring phenomenon in the tropical Pacific, which has global impacts of great relevance to society. The term "El Niño" refers to warming of the tropical Pacific Ocean occurring every 2-7 years, and alternating with the opposite cold phase, known as "La Niña". Anomalous warming or cooling conditions are associated with a large-scale east-west sea level pressure seesaw, termed the "Southern Oscillation", which represents the atmospheric manifestation of the coupled ENSO phenomenon (McPhaden et al. 2006). ENSO events differ in amplitude, temporal evolution, and spatial pattern. While differences among ENSO events have been known for many years, a renewed interest in this diversity was stimulated by Larkin and

62 Harrison (2005) and Ashok et al. (2007), who highlighted an unusual sea surface
63 temperature anomaly (SSTA) pattern over the tropical Pacific during the summer of 2004
64 that was associated with remote impacts on surface air temperature and precipitation
65 different from those related to "typical" El Niño conditions. Because of the similarity and
66 differences from a "typical" El Niño, Ashok et al. (2007) named this pattern El Niño
67 "Modoki" (a Japanese word that means "similar but different") and argued that it is a
68 different type of El Niño. Significant research has since been conducted to identify,
69 describe, and understand these "El Niño types", spurring debates on whether there are
70 indeed two distinct modes of variability, or whether ENSO can be more aptly described
71 as a diverse continuum. In this article, we report on advances in understanding ENSO
72 diversity, drawing from community discussions that took place at the U.S. CLIVAR
73 Workshop on ENSO Diversity held in Boulder, Colorado, during February 6-8, 2013
74 (U.S. CLIVAR ENSO Diversity WG 2013).
75
76 **What is "ENSO diversity"?**
77 A common way to highlight ENSO diversity is to contrast SSTA patterns at the height of
78 different ENSO events. Fig. 1 (right panels) shows boreal winter SSTAs for the 1997-98
79 and 2004-2005 El Niños, as well as 2007-2008 and 1988-89 La Niñas. For 1997-98,
80 SSTAs peak along the western coast of South America, and extend westward along the
81 equator with decreasing amplitude -- a pattern similar to the "canonical" El Niño
82 described by Rasmusson and Carpenter (1982). For 2004-2005, on the other hand, the
83 positive SSTAs are substantially weaker, and peak near the dateline, with no significant
84 warming of the east Pacific cold tongue region. La Niña events, which tend to peak

85 further west than warm events, show subtler inter-event differences in their spatial
86 patterns. For this reason, most of the emphasis in ENSO diversity research has been
87 devoted to warm events. Several indices have been introduced to characterize the
88 differences in the spatial patterns of El Niño and their associated surface and subsurface
89 characteristics (see sidebar "Indices of El Niño diversity"). In the following, we will refer
90 to events resembling the 1997-98 and 2004-05 cases as "Eastern Pacific" (EP), and
91 "Central Pacific" (CP) El Niños, respectively, as termed by Kao and Yu (2009). Note,
92 however, that in this paper these definitions are used as shorthand for a qualitative
93 description, and do not imply a clear dichotomy between EP and CP event types. In fact,
94 when examining the distribution of events in longitude-amplitude phase space (Fig. 1, left
95 panel) we see that both warm and cold events occur over a broad range of longitudes.
96 While some of the events that we define "EP" and "CP" capture the extrema of that
97 distribution, there are also many events that co-mingle in the center. For these events,
98 their identification as "EP" or "CP" depends somewhat on the methodology used. Notice
99 that the strongest events occur in the eastern Pacific, with El Niños having potentially
100 larger amplitude than La Niñas. In the Central Pacific, on the other hand, negative events
101 tend to be a little stronger than positive events. This amplitude asymmetry between
102 positive and negative events, which is itself a function of longitude, may be an indication
103 of nonlinearities in the system (Takahashi et al. 2011; Dommenget et al. 2013; Choi et al.
104 2013; Graham et al. 2014), and represent another important aspect of ENSO diversity.
105
106 Differences in the location and strength of the SSTA maximum correspond to differences
107 in the evolution of each ENSO event. For example, Fig. 2 shows how SSTA patterns

similar to “EP” and “CP” cases (Fig. 2, middle panels) evolve from some initial tropical anomaly pattern, or “precursor”, as shown in the top panels of Fig. 2. In this example, the “precursor” patterns have been determined from observed SSTs, 20ºC isotherm depth, and zonal surface wind stress over the period 1959-2000, by fitting a linear stochastically forced dynamical model to the observations (Penland and Sardeshmukh 1995; Newman et al. 2011a, b). Observed anomalies that have a large projection on one of the “precursor” structures at some given time also have a large projection on the corresponding evolved structure six month later (Fig. 2, bottom panels). However, within this framework, in general ENSO events are neither solely CP nor EP events, but rather different linear combinations of both of these ENSO flavors (color shading in bottom panels of Fig. 2), which themselves result from different balances of physical processes. Some nonlinear processes, not fully captured by the above linear stochastic model, may also play an important role in the evolution of strong events, either EP El Niño or CP La Niña (Jin et al. 2003, Takahashi et al. 2011, Choi et al. 2013, Vecchi et al. 2006), and may differentiate their evolution from weaker events. EP and CP cases also have different seasonal evolutions (Kao and Yu 2009; Yeh et al. 2014). For EP events, SSTAs typically appear in the far eastern Pacific during spring, and extend westward during summer and fall, while in the CP cases anomalies extend from the eastern subtropics to the central Pacific during spring and summer. Both event types achieve their maximum amplitude during boreal winter. The exact onset and evolution of individual events of either type is somewhat dependent on the timing and strength of the high-frequency atmospheric forcing that triggers each event (Karnauskas 2013), as further discussed in the “Predictability and Prediction” section.

131 Understanding ENSO diversity has been hampered by the relatively short duration of the
132 observational record. Marine observations are very sparse for most of the 20th century,
133 with a large increase over the last 30 years (Yu and Giese 2013). Attempts have been
134 made to extend the observational record back in time via "reconstruction" techniques,
135 which often use spatial patterns typical of recent observationally dense periods as basis
136 functions, to project SSTAs into earlier periods with sparse observations. Because these
137 reconstructions (i.e. HadISST, ERSST, Kaplan) rely primarily on the spatial structure of
138 ENSO over the last 30 years, ENSO events in these reconstructions may be biased toward
139 the patterns of recent events, leading to underestimates of the true ENSO diversity (Giese
140 et al. 2010).
141
142 Proxies for tropical Pacific climate, including corals, tree rings, lake sediments, and ice
143 cores from alpine glaciers, provide a longer-term view of equatorial Pacific climate and
144 ENSO variability before the instrumental era (Emile-Geay et al. 2013a, b; McGregor et al.
145 2013). For example, a 7,000-year record from central Pacific corals (Cobb et al. 2013)
146 suggests a strong decadal-to-centennial modulation of ENSO, in qualitative agreement
147 with the amplitude modulation seen in unforced Coupled General Circulation Model
148 (CGCM) simulations (Wittenberg 2009; Stevenson et al. 2012; Deser et al. 2012;
149 Wittenberg et al. 2014). However, relative to proxy reconstructions, unforced CGCMs
150 tend to underestimate tropical multidecadal variability and may be too sensitive to
151 external forcing (Ault et al. 2013). In these central Pacific coral records, the inferred
152 interannual variance over the past 1,000 years is statistically indistinguishable from that
153 during the mid-Holocene (6,000 years ago, or 6ka) -- in contrast to proxy records from

154 the east Pacific (Moy et al. 2002, Convoy et al. 2008), which suggest reduced interannual
155 variability at 6ka, as do mid-Holocene model simulations (Zheng et al. 2008; An and
156 Choi 2013). One interpretation of these proxy results is that ENSO SST variability was
157 displaced westward at 6ka. Indeed, results from a modeling study suggest larger SSTA
158 differences in the eastern Pacific between early and mid-Holocene (Braconnot et al.
159 2012), an indication of potentially greater uncertainty in that region. Thus, paleoclimate
160 research offers a broader view of ENSO diversity, although the sparseness of proxy
161 records and the remaining uncertainties in their interpretation do not yet allow a detailed
162 description of that diversity.
163
164 Ocean reanalyses (e.g. Carton and Giese 2008; Zhang et al. 2007; Sun et al. 2007) can
165 provide an alternative approach to reconstructed data sets, as they do not constrain
166 historical SSTAs to look like the SSTA patterns associated with ENSO in recent years,
167 and use both atmospheric information (surface heat and momentum fluxes) and ocean
168 information (surface and subsurface observations, plus oceanic dynamics simulated by an
169 ocean GCM). For example, a recent version of the Simple Ocean Data Assimilation
170 (SODA, Carton and Giese 2008) has been forced with atmospheric fields (the 20th
171 century reanalysis, Compo et al. 2010) spanning the period 1871-2008, providing a
172 relatively long record for ENSO diversity studies (Giese and Ray 2011) -- albeit still
173 subject to secular changes in the observing system (e.g. for the surface fluxes; Wittenberg
174 2004). Giese and Ray (2011) used the first moment of the equatorial SSTAs (Center of
175 Heat Index, "CHI") to examine the joint distribution of longitude and strength of ENSO
176 events in the 138-year SODA reanalysis. Their analysis focuses on events with near-

177 equatorial SSTAs exceeding 0.5°C in magnitude over an area as large (or larger) than the
178 Niño3.4 region (120°W-170°W, 5°S-5°N). Their results indicate that the CHIs span a
179 broad range of longitudes centered around 140°W, with a distribution that is statistically
180 indistinguishable from Gaussian. The characterization of ENSO diversity based on SST
181 statistics and SST-based indices focuses on the oceanic signature of El Niño and does not
182 necessarily account for the coupled ocean-atmosphere signature of ENSO. Other studies
183 (e.g., Chiodi and Harrison 2013) have considered parameters that are more characteristic
184 of ocean-atmosphere coupling, such as the eastern equatorial Pacific outgoing longwave
185 radiation (OLR). An index combining coupled SSTA and precipitation anomalies may be
186 a good indicator of the most extreme teleconnections of ENSO (Cai et al. 2014).
187
188 Climate models can provide long simulations that include complete surface and
189 subsurface information, to examine ENSO diversity in greater detail. In particular, the
190 Climate Model Intercomparison Project versions 3 and 5 (CMIP3 and CMIP5) include
191 long simulations performed with numerous models, thus allowing the examination of
192 ENSO diversity across a large multi-model ensemble. However, climate models have
193 biases – for example, El Niño SSTA patterns that peak too far west. These biases, found
194 in both the CMIP3 (Capotondi et al. 2006; Capotondi 2010; Guilyardi et al. 2009) and
195 CMIP5 (Guilyardi et al. 2012; Yang and Giese 2013) simulations, are extreme in some
196 models and may limit their ability to reproduce the observed range of ENSO flavors
197 (Ham and Kug 2012). A few models, however, can reproduce ENSO diversity with some
198 realism (Yu and Kim 2010; Kim and Yu 2012), and can provide valuable insights.
199

200 For example, a 4000-year pre-industrial control simulation from the Geophysical Fluid
201 Dynamics Laboratory Climate model version 2.1 (GFDL-CM2.1) captures much of the
202 observed diversity of ENSO, although it significantly overestimates the amplitude of
203 ENSO interannual variability. This simulation has provided a detailed look at the
204 distribution of the model's ENSO events (Delworth et al. 2006; Wittenberg et al. 2006,
205 2014; Wittenberg 2009; Kug et al. 2010). Because this simulation uses unchanging
206 external forcings, its ENSO diversity is entirely intrinsically generated. The scatterplot in
207 Fig. 3 shows the peak DJF SSTA along the equator -- and the corresponding longitude
208 where that peak occurs -- for every warm event in this simulation. The events with west
209 Pacific SSTA peaks are weak, and those with central Pacific peaks are intermediate in
210 strength, in agreement with the observationally-based scatter plot in Fig. 1. Also similar
211 to Fig. 1, the strongest events always peak in the east Pacific, although east Pacific events
212 can exhibit a wide range of amplitudes. While the marginal distribution of CM2.1-
213 simulated peak amplitudes (Fig. 3c) offers no evidence of bimodality, the marginal
214 distribution of peak longitudes (Fig. 3a) does have a weakly bimodal character -- with a
215 tendency for SSTAs to peak most frequently near either 160˚E (albeit farther west than
216 observed) or 115˚W. However, characterizing the simulated warm events as consisting of
217 purely "western" and "eastern" types would be at odds with the bivariate distribution (Fig.
218 3b) -- which actually shows a continuum of events whose peaks shift eastward as they
219 strengthen, plus a smaller group of weak EP events.
220
221 Millennia-long simulations from the GFDL-CM2.1 and the National Center for
222 Atmospheric Research Community Climate System Model Version 4 (NCAR-CCSM4)

223 have allowed a detailed analysis of the leading dynamical processes of events peaking at
224 different longitudes, with results that are consistent with the view of ENSO diversity that
225 has emerged from the shorter observational record. The quasi-cyclic ENSO evolution
226 involves the movement of the upper-ocean warm water volume (WWV) to/from the
227 equatorial thermocline, a process known as "WWV recharge/discharge" (Jin 1997,
228 Meinen and McPhaden 2000). The equatorial thermocline, the layer of large vertical
229 density gradients that separates the warmer and active upper-ocean from the colder deep
230 ocean, is shallower in the eastern Pacific, and deepens westward. Changes in the depth of
231 the thermocline associated with the recharge/discharge processes are more influential on
232 SST in the eastern Pacific, where the thermocline is shallower, than in the western Pacific.
233 Horizontal advection, especially the advection of the large zonal temperature gradients by
234 the anomalous zonal currents, a process known as the "zonal advective feedback", is
235 another key process in the development of SST anomalies associated with ENSO. The
236 zonal advective feedback tends to be more effective in the central Pacific, due to the large
237 mean zonal SST gradients near the edge of the Warm Pool. Thus, the leading dynamical
238 processes differ with event location, with thermocline anomalies and recharge/discharge
239 processes becoming progressively weaker as events peak further west (Kug et al. 2010;
240 Capotondi 2013).
241
242 Fig. 4, for example, shows that for simulated events peaking in the Niño3 region (Fig. 4a)
243 the equatorial thermocline depth anomalies achieve their maximum depth (recharged
244 state) a few months before the peak of the event (Jan 1), and then decrease rapidly
245 afterwards, an indication of the discharge of the warm water volume from the equatorial

246 thermocline to higher latitudes. For events peaking in the Niño4 region (Fig. 4b) the
247 equatorial thermocline undergoes a similar evolution, but much weaker, while for events
248 peaking in the westernmost region (Fig. 4c) the thermocline anomalies are very weak,
249 and remain of the same sign throughout the event evolution, indicating the absence of
250 warm water discharge.
251
252 Zonal advection and air-sea heat fluxes, on the other hand, are relatively more important
253 in the heat budget of the central Pacific SST anomalies, as also found in observational
254 studies (Kao and Yu 2009; Kug et al. 2009, 2010; Yu et al. 2010; Lübbecke and
255 McPhaden 2014; Newman et al. 2011b). In particular, using a variety of reanalysis
256 products, Lübbecke and McPhaden (2014) find a weakening of the thermocline feedback,
257 relative to the zonal advective feedback, in the eastern equatorial Pacific during the CP-
258 dominated 2000-2010 decade.
259
260 **Teleconnections and Impacts**
261 SSTAs associated with the ENSO cycle influence convective processes and modify the
262 atmospheric circulation, thus affecting patterns of weather variability worldwide
263 (Trenberth et al. 1998). These atmospheric teleconnections can be strongly influenced by
264 key details of equatorial SSTA pattern. The atmosphere tends to be most responsive to
265 SSTAs in the Indo-Pacific Warm Pool region, where the surface is warm and atmospheric
266 deep convection is most active, and less sensitive to SSTAs in the eastern Pacific cold
267 tongue. However, SSTAs are stronger in the eastern Pacific, and the combination of

atmospheric sensitivity and SSTA amplitude leads to the central equatorial Pacific playing a key role in remote impacts (Barsugli and Sardeshmukh 2002; Shin et al. 2010).

Through atmospheric teleconnections, ENSO influences the evolution of extratropical modes of atmospheric variability. The strength of the Aleutian Low, the leading mode of north Pacific sea level pressure (SLP) variability, is influenced by SSTAs in both the eastern and central equatorial Pacific (Yu and Kim 2011). SSTAs in the central Pacific, however, have greater impact upon the second mode of North Pacific SLP variability, the North Pacific Oscillation (NPO) at decadal time scales (Di Lorenzo et al. 2010). The NPO is the atmospheric driver of the North Pacific Gyre Oscillation (NPGO), a mode of sea surface height (SSH) and SST variability that is connected with fluctuations of physical quantities (e.g. salinity, nutrients, chlorophyll-A) that are crucial for planktonic ecosystem dynamics in the northeast Pacific (Di Lorenzo et al. 2008).

The influences of tropical Pacific SSTAs associated with ENSO on precipitation and surface air temperatures over many parts of the globe have been outlined in the seminal papers of Ropelewski and Halpert (1987) and Halpert and Ropelewski (1992). Robust features include warm wintertime temperatures over the northern U.S. and western Canada and excess precipitation over the Southeastern U.S. However, CP events in recent years appear to be associated with different temperature and precipitation impacts over the U.S. (Larkin and Harrison 2005, hereafter LH05, Figs. 5 and 6). For example, during the fall season, EP events (defined as “conventional” by LH05) are associated with cooling in the central U.S., while during CP events (“dateline” events in LH05’s

definition) the central U.S. experiences warming. In winter, the large warming in the northwestern U.S. during EP events is absent during CP events. Instead, cooling in the southeastern U.S. is observed (Fig. 5). Similarly, the pattern and even sign of precipitation anomalies over the U.S. differ for the two event types (Fig. 6). However, the patterns shown in Figs. 5 and 6 are based on a relatively small number of cases, so that large uncertainties remain on the temperature and precipitation anomalies patterns associated with the EP and CP events, and their differences.

El Niño events have also been associated with reduced precipitation over northern, central and peninsular India (Rasmusson and Carpenter 1983, Shukla and Paolino 1983, Ropelewski and Halpert 1987), as well as northern and eastern Australia (Wang and Hendon 2007, Cai and Cowan 2009, Taschetto and England 2009). The location of SSTAs along the equatorial Pacific appears to be the most important factor for the reduced precipitation over both India and Australia, with events peaking in the central Pacific being much more influential than strong events peaking in the eastern Pacific. Thus, moderate El Niño events, like the 2002 and 2004 CP events, have resulted in severe and economically devastating droughts in both India (Kumar et al. 2006) and Australia (Wang and Hendon 2007), while the very strong 1997-1998 El Niño had very little effect on precipitation in both regions. La Niña events are associated with increased precipitation over Australia, with marked differences between EP and CP types (Cai and Cowan 2009).

313 The large influence of CP El Niños on Southern Hemisphere wintertime storm track
314 activity (Ashok et al. 2007) appears to have important impacts on temperature anomalies
315 over Antarctica (Lee et al. 2010). The location of SSTAs has also implications for the
316 frequency and trajectory of North Atlantic tropical cyclones. Cyclone activity is usually
317 reduced during El Niño, and enhanced during La Niña. However, warming in the central
318 Pacific has been associated with an increased frequency of North Atlantic tropical
319 cyclones, with enhanced likelihood of landfall along the Gulf of Mexico and Central
320 America (Kim et al. 2009).
321
322 Apart from extra-tropical influences, the different spatial patterns of SSTAs during EP
323 and CP events have large socioeconomic consequences in the tropics (McPhaden 2004).
324 During large EP El Niño events, warming in the eastern Pacific leads to a southward shift
325 of the Intertropical Convergence Zone, resulting in intense rainfall over eastern Pacific
326 regions that are normally dry, with greater incidence of catastrophic floods in parts of
327 Ecuador and northern Peru. In contrast during CP events, cooler conditions can exist in
328 the eastern Pacific (Dewitte et al. 2012), producing dryness in Peru and Ecuador during
329 the usual rainy season, with disruptions to local agriculture.
330
331 The ocean circulation changes associated with different ENSO types have distinct
332 impacts on biological processes along the equator. Classical EP El Niños are known to
333 reduce eastern Pacific chlorophyll-A concentrations, by deepening the ocean thermocline
334 and weakening the upwelling of nutrient-rich deep waters in that region. CP El Niños
335 cause similar biological changes in the central Pacific rather than in the eastern Pacific

(Turk et al. 2011; Radenac et al. 2012), but for different reasons -- namely stronger horizontal advection of nutrient-depleted Warm Pool waters toward the central equatorial Pacific (Gierach et al. 2012, Lee et al. 2014). Along the western coast of South America, CP and EP El Niños have been shown to have significantly different impacts on the upwelling off Peru, with a tendency for colder SST during CP El Niño events (Dewitte et al. 2012). Decadal variations in the relative frequency of EP and CP events would be expected to produce a restructuring of the marine ecosystems, with important implications for fisheries.

Predictability and Prediction

Predictability of ENSO events in general, and specific types in particular, relies on the existence of precursors or "triggers" (atmospheric and/or oceanic) responsible for the excitation of events at some lead time. Precursors within the equatorial Pacific are in the form of intra-seasonal atmospheric disturbances known as Westerly Wind Events (WWEs) or Westerly Wind Bursts (WWBs, McPhaden 1999, McPhaden and Yu 1999, Fedorov 2002). WWEs occur near the dateline, and can excite eastward propagating Kelvin waves which, in turn, favor the development of El Niño by deepening the eastern equatorial Pacific thermocline, creating positive SSTAs in the eastern Pacific, and leading to a weakening of the trade winds and to a further deepening of the thermocline, a positive feedback known as the Bjerknes feedback. The timing, strength, and longitudinal location of the WWEs appear to be very important in the development of either EP or CP events (Karnauskas 2013; Harrison and Chiodi 2009). While the efficiency of WWEs in triggering El Niño events has been documented from observations (McPhaden and Yu

359 1999), the short duration of the instrumental record does not allow a full understanding of
360 the mechanistic link between ENSO and WWEs.
361
362 Recent numerical experiments have also highlighted the importance of the ocean
363 background conditions in determining the type of El Niño resulting from WWEs activity.
364 If the tropical Pacific upper-ocean heat content is larger than normal, a condition referred
365 to as a "recharged state", WWEs can lead to an EP El Niño (Lengaigne et al. 2004), while
366 for upper ocean heat content levels that are near average ("neutral") WWEs may result in
367 a CP El Niño (Fedorov et al. 2014). WWE prevalence, in turn, depends on the zonal
368 extent of the west Pacific warm pool -- which is a function of both the background
369 climatological state and ENSO (Eisenman et al. 2005; Vecchi et al. 2006). This could
370 result in a coupled, nonlinear interplay among the WWEs, ENSO, and the decadal
371 background state (Gebbie et al. 2007; Zavala-Garay et al. 2008; Sun and Yu 2009;
372 Harrison and Chiodi 2009; Ogata et al. 2013; Choi et al. 2013).
373
374 Off-equatorial atmospheric variability can also play an important role in triggering ENSO
375 events. In particular, the NPO is associated with wind anomalies that impart a "footprint"
376 on the ocean through changes in surface heat fluxes. The SST footprint, which is termed
377 the North Pacific Meridional Mode (NPMM) because of its association with a subtropical
378 north-south SST gradient that peaks in spring and persists through summer (Chiang and
379 Vimont 2004, Chang et al. 2007), has been shown to trigger ENSO events (Larson and
380 Kirtman 2013). This mode exerts a positive feedback that further weakens the winds and
381 strengthens the existing SSTAs. This positive SST feedback, known as the wind-

382 evaporation-SST (WES) feedback (Xie 1999) supports a southwestward co-evolution of
383 the oceanic SSTAs and wind anomalies that ultimately reaches the tropics, favoring the
384 development of an El Niño event by weakening the Walker circulation.
385
386 Apart from this thermodynamic coupling, the NPO-related wind anomalies can
387 dynamically energize equatorial processes through the excitation of off-equatorial Rossby
388 waves (Alexander et al. 2010), as well as changes in the strength of the tropical upper-
389 ocean overturning circulation (Anderson et al. 2013). This NPO-related forcing has been
390 associated with CP events (Yu and Kim 2011, Kim et al. 2012; Vimont et al. 2014). As
391 for the WWEs, the selection of the type of ENSO response may depend upon the mean
392 state of the equatorial ocean, whether recharged, neutral, or discharged (Anderson 2007,
393 Alexander et al. 2010, Deser et al. 2012).
394
395 An SSTA pattern similar to the NPMM exists also in the Southern Hemisphere, and has
396 been termed the South Pacific Meridional Mode (SPMM) by Zhang et al. (2014).
397 Although similar in nature to the NPMM, the SPMM extends all the way to the eastern
398 and central equatorial Pacific, while the NPMM is limited to the Northern Hemisphere
399 subtropics. It is possible that the SPMM is more effective in exciting eastern Pacific
400 events, while the NPMM may be more effective in triggering central Pacific events
401 (Zhang et al. 2014; Vimont et al. 2014).
402
403 As the existence of possible precursors indicates some seasonal-to-interannual
404 predictability of the various ENSO flavors, the ability of state-of-the-art prediction

405 systems to capture ENSO diversity has been examined in the North American Multi-
406 Model Ensemble (NMME) prediction experiment (Kirtman et al. 2013). The NMME
407 system includes ensemble retrospective forecasts (1982-present) from nine different
408 models. For lead-times up to six months and from a qualitative basin-scale perspective,
409 the models are able to capture some of the observed contrasts between the warming in the
410 east versus west Pacific and the associated differences in the rainfall anomalies. However,
411 the models systematically produce too much warming in the east compared to the
412 observational estimates for events centered in the central/western Pacific, so that the
413 strong eastern Pacific events are demonstrably better predicted at both short and long lead
414 times.
415
416 ENSO prediction skill at more than three months lead time largely originates from the
417 oceanic memory associated with the equatorial Pacific upper ocean heat content. The
418 Warm Water Volume (WWV) index, defined as the average depth of the 20°C isotherm
419 in the equatorial band, has been shown to be a good predictor of ENSO events 2-3
420 seasons in advance (Meinen and McPhaden 2000). The changes in the recharge-discharge
421 processes associated with the higher frequency of CP events since 2000 has reduced the
422 role of the WWV index as a predictor (Hendon et al. 2009, McPhaden 2012), and
423 degraded the predictive skills of seasonal forecast models for the 2002-2011 period
424 relative to the 1980s and 1990s (Wang et al. 2010, Barnston et al. 2012, Xue et al. 2013).
425
426 On longer time scales, observations and climate simulations exhibit epochs of extreme
427 ENSO behavior that can persist for decades (e.g. Wittenberg 2009; Stevenson et al. 2012;

McGregor et al. 2013; Cobb et al. 2013; Karamperidou et al. 2014). Model simulations suggest that epochs with an abundance of strong, EP-type El Niños tend to be associated with decadally warm conditions in the east Pacific, and decadally cooler conditions in the west (Choi et al. 2011, 2012), which may in large part be due to the rectification of the ENSO signal (Rodgers et al. 2004; Schopf and Burgman 2006; Ogata et al. 2013). The extent to which decadal variations (either intrinsic to the climate system, or ENSO-driven) affect ENSO behavior is not yet clear. Experiments with the GFDL-CM2.1 control simulation (Wittenberg et al. 2014), in which the model's own multi-decadal epochs of extreme ENSO behavior were reforecast using a "perfect model" setup with only tiny perturbations to the initial conditions, indicated no inherent decadal-scale predictability of ENSO behavior (amplitude, frequency, or type) – suggesting that in the absence of changes in external forcings, such multi-decadal extreme epochs could occur at random.

ENSO Diversity and Climate Change

The abundance of events with SSTAs peaking in the central Pacific over the last twenty years (Lee and McPhaden 2010), as compared to prior decades, has been suggested as a possible harbinger of changes in ENSO characteristics due to global warming (Yeh et al. 2009). Indeed, the ratio of CP to EP type events (at least in terms of *SST* patterns) is projected to increase in the CMIP3 climate model simulations under global warming scenarios (Yeh et al. 2009), with similar results for the CMIP5 simulations (Kim and Yu 2012). Climate models project a weakening of the climatological Walker circulation as a result of global warming (Vecchi et al. 2006; Xie et al. 2010), with a consequent

451 weakening of the zonal slope of the equatorial thermocline, and a weaker eastern
452 equatorial Pacific cold tongue. [However, it remains unclear whether the Walker
453 circulation has in fact weakened, stayed the same, or even strengthened in recent decades
454 (e.g., Solomon and Newman 2012; L'Heureax et al. 2013; Sandeep et al. 2014).] These
455 changes have been suggested as possible drivers of the recent increase in the occurrence
456 of CP type events. While the weakened trade winds and weakened equatorial upwelling
457 reduce ENSO SSTAs in the eastern Pacific (by reducing the thermocline feedback), the
458 increased thermal stratification of the sloping thermocline enhances ENSO SSTAs in the
459 central Pacific, by strengthening both subsurface zonal advective feedbacks (DiNezio et
460 al. 2012) and thermocline feedbacks (Dewitte et al. 2013) in that region. Interestingly,
461 extreme El Niño events in terms of equatorial *rainfall* patterns, resembling the 1982-83
462 and 1997-98 cases, are also projected to increase in frequency due to global warming
463 (Cai et al. 2014).
464
465 So far the impact of climate change on ENSO diversity has been difficult to evaluate,
466 given that ENSO behavior may be intrinsically modulated even in the absence of external
467 forcing (Zebiak and Cane 1987; Wittenberg 2009). The random combinations of initial
468 optimal structures obtained with a linear stochastic model (Newman et al. 2011a; Fig. 2,
469 top panels) can produce extended epochs dominated by either type of event, without the
470 need for anthropogenic changes in the background state. This behavior is also seen in
471 coupled GCMs, where unforced control runs can spontaneously generate multi-decade
472 epochs populated entirely by CP or EP events (Kug et al. 2010; Choi et al. 2011;
473 Wittenberg et al. 2014).

474

475 This intrinsic modulation of ENSO can in turn affect the multi-decadal background state,
476 confounding detection of anthropogenic influences in short climate records. In unforced
477 climate simulations, epochs with greater incidence of the weaker, CP-like El Niños
478 appear to steepen the equatorial time-mean thermocline slope and zonal SST gradient
479 (Rodgers et al. 2004; Ogata et al. 2013). Indeed an analysis of SST observations over the
480 past three decades (Lee and McPhaden 2010) suggests that the increasing amplitude of El
481 Niño in the central Pacific contributed to the well-observed multi-decadal warming in this
482 region, thus enhancing the zonal SST gradient. In addition, McPhaden et al. (2011)
483 showed from observations that the equatorial thermocline steepened in moving from
484 1980-1999 (when EP events prevailed) to 2000-2010 (when CP events prevailed). This
485 would seem to contrast with the anthropogenic response described above, in which a
486 weakened time-mean zonal SST gradient, and a flatter but more intense thermocline,
487 favor CP events. However, given the substantial remaining uncertainty regarding the
488 magnitude (and even the sign) of the anthropogenic impacts and of ENSO's interactions
489 with the mean state (Vecchi and Wittenberg 2010; Collins et al. 2010; Compo and
490 Sardeshmukh 2010;DiNezio et al. 2010, 2012; Solomon and Newman 2012; Tokinaga et
491 al. 2012a,b), it is not yet clear to what extent observed ENSO modulation is a cause or a
492 consequence of either anthropogenic or intrinsic decadal-scale changes in the equatorial
493 Pacific mean state.

494

495

496 **Conclusions**

497 The last decade has seen exciting advances in ENSO research. Differences among ENSO
498 events, although recognized for a long time, have been examined in greater depth, and it
499 has become increasingly clear that the details of the spatial patterns associated with
500 ENSO affect its atmospheric teleconnections and impacts. Examinations of observations,
501 climate reanalyses, and climate models show that while the essential physical processes
502 underlying the different ENSO types are the same, their relative roles may vary in driving
503 SSTAs at different longitudes. For example, the thermocline feedback is more effective at
504 driving SSTAs in the eastern Pacific, where the thermocline is closer to the surface, while
505 zonal advection near the edge of the Warm Pool is most effective at driving SSTAs in the
506 central Pacific. Strong events, which usually peak in the eastern Pacific, may also involve
507 nonlinear processes. Thus, ENSO can be described as a coupled atmosphere-ocean
508 phenomenon that exhibits substantial variations with regionally different feedbacks,
509 leading to a diverse continuum of realized ENSO events.
510
511 As our understanding of ENSO broadens, new questions arise:
512
513 1. How is ENSO diversity influenced by decadal-to-centennial scale changes in
514 radiative forcings and the climatological background state?
515 2. What are the sources and limits of predictability, both tropical and extratropical,
516 associated with the differences in ENSO events?
517 3. Do climate models properly represent ENSO diversity?
518 4. Can we improve forecasts of ENSO flavors in operational ENSO prediction
519 systems?

To answer these questions, further studies are needed using observational and reanalysis data sets, paleoclimate records, and model simulations. Sustained and enhanced climate observations, better models, and improved understanding are all imperative for more reliable ENSO monitoring and prediction in a changing climate.

Sidebar

Indices of El Niño diversity

To better understand ENSO diversity, several indices have been introduced to identify different event types, with emphasis on the warm (El Niño) ENSO phase. Indices have been constructed from SST (a-d), subsurface ocean temperature (e), sea surface salinity (f), or OLR anomaly information (g). Definitions of El Niño types often vary with the method used.

a) Niño3-4 index method (Kug et al. 2009; Yeh et al. 2009): An El Niño event is classified as a "Warm Pool" type if its SSTA averaged over the Niño4 region (160°E-150°W, 5°S-5N) exceeds one standard deviation, and exceeds the SSTA averaged over the Niño3 region (90°W-150°W, 5°S-5°N). "Cold Tongue" events are characterized by Niño3 SSTA exceeding one standard deviation, and exceeding the Niño4 SSTA.

b) El Niño Modoki Index (EMI) method (Ashok et al. 2007): This index is constructed as the difference between SSTA averaged over the central Pacific(165°E-140°W, 10°S-10°N), and SSTA averaged over the western (125°E-145°E, 10°S-20N) and eastern

542 (110°W-70°W, 15°S-5°N) Pacific, to emphasize the out-of-phase relationship between
543 SSTA in the central Pacific versus the eastern/western Pacific.
544
545 **c) EP/CP-Index method (Kao and Yu 2009; Yu et al. 2012):** Regression of SSTA onto
546 the Niño1+2 index (average SSTA over the region 0°-10°S, 90°W-80°W) is used to
547 remove the SSTA component associated with east Pacific warming, and then a principal
548 components analysis (PCA) is used to determine the spatial pattern and associated
549 temporal index of the CP events. Similarly, regression of SSTA onto the Niño4 index is
550 used to remove the SSTA component associated with central Pacific warming, and then
551 PCA is used to determine the pattern and index of the EP events. A related approach uses
552 the Niño3 index to identify EP events, and uses the leading principal component of
553 tropical Pacific SSTA (after removal of the SSTA regression onto the Niño3 index) to
554 identify Central Pacific Warming (CPW) events (Di Lorenzo et al. 2010).
555
556 **d) E and C indices (Takahashi et al., 2011)**: This method uses two orthogonal axes that
557 are rotated 45° relative to the principal components of SSTA in the tropical Pacific. The
558 associated projections of the SSTA onto these rotated axes provides the E-index
559 (representing the Eastern Pacific El Niño) and the C-index (representing both the Central
560 Pacific El Niño, and La Niña events).
561
562 **e) EP/CP Subsurface Index method (Yu et al. 2011)**: CP El Niños produce their
563 largest subsurface temperature anomalies in the central Pacific, where EP El Niños
564 exhibit only weak subsurface anomalies. With this method, temperature anomalies for the

top 100m of the ocean are averaged over the eastern and central equatorial Pacific, respectively, to construct EP and CP indices.

f) Sea Surface Salinity (SSS) Index method (Singh et al. 2011; Qu and Yu 2014): SSS anomaly distributions differ among different El Niño events. SSS indices were defined utilizing these differences in the western-to-central equatorial Pacific (Singh et al. 2011) and in the southeastern Pacific (Qu and Yu 2014) to distinguish El Niño types.

g) Outgoing Longwave radiation (OLR)-Index method (Chiodi and Harrison 2013): An index was constructed using OLR anomalies over the eastern-to-central equatorial Pacific, to separate events into El Niños characterized by an OLR signal, and those without an OLR signal. The two classes of events so identified were found to produce different remote climate impacts.

Acknowledgments. The authors of this paper are members of the US CLIVAR ENSO Diversity Working Group, sponsored by US CLIVAR. The Working Group wishes to acknowledge the US CLIVAR office for its support, and the US CLIVAR funding agencies, NASA, NOAA, NSF, and DoE, for their sponsorship.

References

Alexander, M. A., D. J. Vimont, P. Chang, and J. D. Scott, 2010: The impact of extratropical atmospheric variability on ENSO: Testing the seasonal footprinting mechanism using coupled model experiments. *J. Climate*, **23**, 2885-2901

588 An, S.-I., and J. Choi, 2013: Mid-Holocene Tropical Pacific Climate State, Annual Cycle,
589 and ENSO in PMIP2 and PMIP3. *Clim. Dyn*.
590 Anderson, B.T., 2007: Intra-seasonal atmospheric variability in the extra-tropics and its
591 relation to the onset of tropical Pacific sea surface temperature anomalies. J. Climate,
592 20, 1593-1599
593 Anderson, B.T., R. Perez, and A. Karspeck, 2013: Triggering of El Niño onset through
594 the trade-wind induced charging of the equatorial Pacific. Geophys. Res. Lett., 40,
595 1212-1216.
596 Ashok, K., S.K. Behera, S.A. Rao, H. Weng, and T. Yamagata, 2007: El Niño Modoki and
597 its possible teleconnections. J. Geophys. Res., 112, C11007,
598 doi:10.1029/2006JC003798
599 Ault, T., C. Deser, M. Newman, and J. Emile-Geay, 2013: Characterizing decadal to
600 centennial variability in the equatorial Pacific during the last millennium. Geophys.
601 Res. Lett, 40, 3450-3456, doi:10.1002/grl.50647.
602 Barnston, A. G., M. K. Tippett, M. L. L'Heureux, S. Li, and D. G. DeWitt, 2012: Skill of
603 real-time seasonal ENSO model predictions during 2002–11: Is our capability
604 increasing? Bull. Amer. Meteor. Soc., 93, 631–651
605 Barsugli, J.j., and P. Sardeshmukh, 2002: Global atmospheric sensitivity to tropical SST
606 anomalies throughout the Indo-Pacific basin. J. Climate, 15, 3427-3442
607 Braconnot, P., Luan, Y., Brewer, S. and Zheng, W.,2012: Impact of Earth's orbit and
608 freshwater fluxes on Holocene climate mean seasonal cycle and ENSO characteristics.
609 *Climate Dynamics*. **38,** 1081-1092.

610 Cai, W., and T. Cowan, 2009: La Niña Modoki impacts Australia autumn rainfall
611 variability. Geophys. Res. Lett., 36, L12805, doi:10.1029/2009GL037885.
612 Cai, W., S. Borlace, M. Lengaigne, P. van Rensch, M. Collins, G. Vecchi, A.
613 Timmermann, A. Santoso, M. J. McPhaden, L. Wu, M. H. England, G. Wang, E.
614 Guilyardi, and F.-F. Jin, 2014: Increasing frequency of extreme El Niño events due to
615 greenhouse warming. Nature Climate Change, doi:10.1038/nclimate2100
616 Capotondi, A., 2010: ENSO ocean dynamics: Simulation by coupled general circulation
617 models. "Climate Dynamics: Why does climate vary?", AGU Monograph Series, D.-
618 Z. Sun and F. Bryan Editors, pp. 53-64.
619 Capotondi, A., 2013: ENSO diversity in the NCAR CCSM4 climate model. J. Geophys.
620 Res., 118, 4755-4770
621 Capotondi, A., A.T. Wittenberg, and S. Masina, 2006: Spatial and temporal structure of
622 tropical Pacific interannual variability in 20th century climate simulations, *Ocean*
623 *Modeling*, **15**, 274-298.
624 Carton, J.A., and B.S. Giese, 2009: A reanalysis of ocean climate using Simple Ocean
625 Data Assimilation (SODA). Mon. Wea. Rev., 136, 2999-3017.
626 Chang, P., L. Zhang, R. Saravanan, D. J. Vimont, J. C. H. Chiang, L. Ji, H. Seidel,
627 and M. K. Tippett, 2007: Pacific meridional mode and El Niño–Southern
628 Oscillation. *Geophys. Res. Lett*., **34**, L16608. doi:10.1029/2007GL030302
629 Chiang, J.C.H., and D.J. Vimont, 2004: Analogous Pacific and Atlantic meridional
630 modes of tropical atmosphere.ocean variability. *J. Climate*, **17**, 4143-4158

631 Chiodi, A. M., and D. E. Harrison, 2013: El Niño impacts on seasonal U.S. atmospheric
632 circulation, temperature, and precipitation anomalies: The OLR-event perspective. J.
633 Climate, 26, 822–837. doi: 10.1175/JCLI-D-12-00097.1
634 Choi, J., S.-I. An, J.-S. Kug, and S.-W. Yeh, 2011: The role of mean state on changes in
635 El Nino flavor. *Clim. Dyn*., **37**, 1205-1215. DOI:10.1007/s00382-010-0912-1
636 Choi, J. S.-I. An, and S.-W. Yeh, 2012: Decadal amplitude modulation of two types of
637 ENSO and its relationship with the mean state. Clim. Dyn., 28, 2631-2644.
638 DOI:/10.1007/s00382-011-1186-y.
639 Choi, K.-Y., G. A. Vecchi, and A. T. Wittenberg, 2013: ENSO transition, duration and
640 amplitude asymmetries: Role of the nonlinear wind stress coupling in a conceptual
641 model. J. Climate, 26, 9462-9476. doi: 10.1175/JCLI-D-13-00045.1
642 Cobb, K.M., N. Westphal, H. Sayani, E. Di Lorenzo, H. Cheng, R.L. Edwards, and C.D.
643 Charles, 2013: Highly variable El Niño-Southern Oscillation throughout the Holocene.
644 *Science*, doi:10.1126/science.1228246.
645 Collins, M., S.-I. An, W. Cai, A. Ganachaud, E. Guilyardi, F.-F. Jin, M. Jochum, M.
646 Lengaigne, S. Power, A. Timmermann, G. Vecchi, and A. Wittenberg, 2010: The
647 impact of global warming on the tropical Pacific and El Niño. Nature Geoscience, 3,
648 391-397. doi: 10.1038/ngeo868
649 Compo, G., and P.D. Sardeshmukh, 2010: Removing ENSO-related variations from the
650 climate record. J. Climate, 23, 1957-1978. DOI: 10.1175/2009JCLI2735.1
651 Convoy, J.L., J.T. Overpeck, J.E. Cole, T.M. Shanahan, M. Steinitz-Kannan, 2008:
652 Holocene changes in eastern tropical Pacific climate inferred from a Galápagos lake
653 sediment record. Quaternary Science Reviews, 27, 1166-1180.

654 Delworth, T. L., et al., 2006: GFDL's CM2 global coupled climate models, Part I:
655 Formulation and simulation characteristics. J. Climate, 19, 643-674. doi:
656 10.1175/JCLI3629.1
657 Deser, C., A. S. Phillips, R. A. Tomas, Y. Okumura, M. A. Alexander, A. Capotondi, J. D.
658 Scott, Y. -O. Kwon, and M. Ohba, 2012. ENSO and Pacific Decadal Variability in
659 Community Climate System Model Version 4. *J. Climate*, **25**, 2622-2651
660 Dewitte B., J. Vazquez-Cuervo, K. Goubanova, S. Illig, K. Takahashi, G. Cambon, S.
661 Purca, D. Correa, D. Gutierrez, A. Sifeddine and L. Ortlieb, 2012: Change in El Niño
662 flavours over 1958-2008: Implications for the long-term trend of the upwelling off
663 Peru. *Deep Sea Research II,* doi:10.1016/j.dsr2.2012.04.011
664 Dewitte, B., S.-W. Yeh, and S. Thual, 2013: Reinterpreting the thermocline feedback in
665 the western-central equatorial Pacific and its relationship with the ENSO modulation.
666 Climate Dynamics, 41, 819-830.
667 Di Lorenzo, E., N. Schneider, K.M. Cobb, P.J.S. Franks, A.J. Miller, J.C. McWilliams,
668 S.J. Bograd, H. Arango, E. Curchitser, T.M. Powell, and P. Riviere, 2008: North
669 Pacific Gyre Oscillation links ocean climate and ecosystem change. *Geophys. Res.*
670 *Lett*., **35**, L08607, doi:10.1029/2007GL032838.
671 Di Lorenzo, K. M. Cobb, J. C. Furtado, N. Schneider, B. T. Anderson, A. Bracco, M. A.
672 Alexander, and D. J. Vimont, 2010: Central Pacific El Niño and decadal climate
673 change in the North Pacific Ocean. *Nature-Geoscience*, **17**, DOI:10.1038/NGEO0984
674 Di Lorenzo, E., K.M. Cobb, B. Anderson, J. Furtado, Z. Ke, N. Schneider, M. Newman,
675 and M. Alexander, 2014: ENSO and the Pacific Meridional Mode: A null-hypothesis
676 for tropical decadal variability. In preparation.

677 Di Nezio, P.N., A.C. Clement, and G.A. Vecchi, 2010: Reconciling differing views of
678 tropical Pacific climate change. Eos, Trans. AGU, 91 (16), 141-142.
679 Di Nezio, P. N., B. P. Kirtman, A. C. Clement, S.-K. Lee, G. A. Vecchi, and A.
680 Wittenberg, 2012: Mean climate controls on the simulated response of ENSO to
681 increasing greenhouse gases. J. Climate, 25, 7399-7420. doi: 10.1175/JCLI-D-11-
682 00494.1
683 Di Nezio, P. N., G. A. Vecchi, and A. C. Clement, 2013: Detectability of changes in the
684 Walker circulation in response to global warming. J. Climate, 26, 4038–4048. doi:
685 10.1175/JCLI-D-12-00531.1
686 Dommenget, D., T. Bayr, and C. Frauen, 2013: Analysis of the non-linearity in the
687 pattern and time evolution of El Niño Southern Oscillation. Climate Dyn., 40, 2825-
688 2847.
689 Eisenman, Ian, Lisan Yu, Eli Tziperman, 2005: Westerly wind bursts: ENSO's tail rather
690 than the dog?. J. Climate, 18, 5224–5238. doi: 10.1175/JCLI3588.1
691 Emile-Geay, J., K. Cobb, M. Mann, and A. T. Wittenberg, 2013a: Estimating central
692 equatorial Pacific SST variability over the past millennium. Part I: Methodology and
693 validation. J. Climate, 26, 2302-2328. doi: 10.1175/JCLI-D-11-00510.1
694 Emile-Geay, J., K. Cobb, M. Mann, and A. T. Wittenberg, 2013b: Estimating central
695 equatorial Pacific SST variability over the past millennium. Part II: Reconstructions
696 and implications. J. Climate, 26, 2329-2352. doi: 10.1175/JCLI-D-11-00511.1
697 Fedorov, A.V., 2002: The response of the coupled tropical ocean-atmosphere to westerly
698 wind bursts. Q. J. Roy. Meteorol. Soc., 128, 1-23.

699 Fedorov, A.V., S. Hu, M. Lengaigne, and E. Guilyardi, 2014: Central Pacific, Eastern
700 Pacific and extreme El Niño events: Dynamics and the role of westerly wind bursts.
701 Climate Dyn., in preparation
702 Gebbie, G., I. Eisenman, A. Wittenberg, and E. Tziperman, 2007: Modulation of westerly
703 wind bursts by sea surface temperature: A semistochastic feedback for ENSO. J.
704 Atmos. Sci., 64, 3281-3295. doi: 10.1175/JAS4029.1
705 Giese, B.S., N.C. Slowey, S. Ray, G.P. Compo, P.D. Sardeshmukh, J.A. Carton, J.S.
706 Whitaker, 2010: The 1918/19 El Niño. Bull. Amer. Meteor. Soc., 91 (2), 177-183.
707 Giese, B.S., and S. Ray, 2011: El Niño variability in simple ocean data assimilation
708 (SODA), 1871-2008. J. Geophys. Res., 116, C02024.
709 Gierach, M.M., T. Lee, D. Turk, and M.J. McPhaden, 2012: Biological response to the
710 1997-98 and 2009-10 El Niño events in the equatorial Pacific Ocean. Geophys. Res.
711 Lett., 39, L10602, doi:10.1029/2012GL051103
712 Graham, F. S., J. N. Brown, C. Langlais, S. J. Marsland, A. T. Wittenberg, and N. J.
713 Holbrook, 2014: Effectiveness of the Bjerknes stability index in representing ocean
714 dynamics. Climate Dyn., published online. doi: 10.1007/s00382-014-2062-3
715 Guilyardi, E., A. Wittenberg, A. Fedorov, M. Collins, C. Wang, A. Capotondi, G. J. van
716 Oldenborgh, and T. Stockdale, 2009: Understanding El Niño in ocean-atmosphere
717 general circulation models: Progress and challenges. Bull. Amer. Meteor. Soc., 90,
718 325-340. doi: 10.1175/2008BAMS2387.1
719 Guilyardi, E., W. Cai, M. Collins, A. Fedorov, F.-F. Jin, A. Kumar, D.-Z. Sun, and A.
720 Wittenberg, 2012: New strategies for evaluating ENSO processes in climate models.
721 Bull. Amer. Met. Soc., 93, 235-238. doi: 10.1175/BAM S-D-11-00106.1

722 Guilyardi, E., H. Bellenger, M. Collins, S. Ferrett, W. Cai, and A. Wittenberg, 2012: A
723 first look at ENSO in CMIP5. CLIVAR Exchanges, 17, 29-32. ISSN: 1026-0471
724 Halpert, M.S., and C.F. Ropelewski, 1992: Surface temperature patterns associated with
725 the Southern Oscillation. J. Climate, 5, 577-593.
726 Ham, Y.-G, and J.-S. Kug, 2012: How well do current climate models simulate two-types
727 of El Nino? *Clim. Dyn*., 39, 383-398. DOI:10.1007/s00382-011-1157-3
728 Harrison, D. E., and A. M. Chiodi, 2009: Pre- and post-1997/98 westerly wind events and
729 equatorial Pacific cold tongue warming. J. Climate, 22, 568–581. doi:
730 10.1175/2008JCLI2270.1
731 Hendon, H.H., E. Lim, G. Wang, O. Alves, and D. Husdon, 2009: Prospects for
732 predicting two flavors of El Niño. Geophys. Res. Lett., 36, L19713,
733 doi:10.1029/2009GL040100.
734 Jin, F.-F., 1997: An equatorial ocean recharge paradigm for ENSO. Part I: Conceptual
735 model. J. Atmos. Sci., 54, 811-829.
736 Jin, F.-F., S.-I. An, A. Timmermann, and J. Zhao, 2003: Strong El Niño events and
737 nonlinear dynamical heating. Geophys. Res. Lett., 30, 1120,
738 doi:10.1029/2002GL016356
739 Kalnay, E., and co-Authors, 1996: the NCEP/NCAR 40-year reanalysis project. Bull. Am.
740 Meteorol. Soc., 77, 437-471.
741 Kao, H. Y., and J. Y. Yu, 2009: Contrasting Eastern-Pacific and Central-Pacific Types of
742 ENSO. *J. Climate*, **22**, 615-632

743 Karamperidou, C., M. A. Cane, U. Lall, and A. T. Wittenberg, 2014: Intrinsic modulation
744 of ENSO predictability viewed through a local Lyapunov lens. Climate Dyn., 42,
745 253-270. doi: 10.1007/s00382-013-1759-z.
746 Karnauskas, K. B., 2013: Can we distinguish canonical El Niño from Modoki? *Geophys.*
747 *Res. Lett.*, **40**, 5246–5251.
748 Kim, H.-M., P.J. Webster, and J.A. Curry, 2009: Impact of shifting patterns of Pacific
749 Ocean warming on North Atlantic tropical cyclones. Science, 325,
750 doi:10.1126//Science.1174062
751 Kim, J.-S., K.-Y. Kim and S.-W. Yeh, 2012: Statistical evidence for the natural variation
752 of the central Pacific El Nino. *J. Geophy. Res*., **117**, C06014,
753 doi:10.1029/2012JC008003
754 Kim, S. T. and J.-Y. Yu, 2012: The Two Types of ENSO in CMIP5 Models*, Geophysical*
755 *Research Letters*, **39**, L11704, doi:10.1029/2012GL052006
756 Kirtman, B.P, and co-authors, 2013: The North American Multi-Model Ensemble
757 (NMME) for Intra-Seasonal to Interannual Prediction. *Bull. Amer. Met. Soc*.,
758 submitted
759 Kug, J.-S., F.-F. Jin, and S.-I. An, 2009: Two types of El Niño events: cold tongue El
760 Niño and warm pool El Niño. *J. Climate.* **22**, 1499–1515
761 Kug, J.-S., J. Choi, S.-I. An, F.-F. Jin, and A. T. Wittenberg, 2010: Warm pool and cold
762 tongue El Niño events as simulated by the GFDL CM2.1 coupled GCM. J. Climate,
763 23, 1226-1239. doi: 10.1175/2009JCLI3293.1
764 Kumar, K.K., B. Rajagopalan, M. Hoerling, G. Bates, and M. Cane, 2006: Unraveling the
765 mystery of Indian monsoon failure during El Niño. Science, 314, 115-118.

766 Larkin, N. K., and D.E., Harrison ,2005: On the definition of El Niño and associated
767 seasonal average U.S. weather anomalies. Geophys. Res. Lett. 32, L13705,
768 doi:10.1029/2005GL022738.
769 Larson, S., and B. P. Kirtman, 2013: The Pacific meridional mode as a trigger for ENSO
770 in a high-resolution coupled model. Geophys. Res. Lett., DOI: 10.1002/grl.50571
771 Lee, T., and M.J. McPhaden, 2010: Increasing intensity of El Niño in the central-
772 equatorial Pacific. Geophys. Res. Lett., 37, L14603, doi:10.1029/2010GL044007
773 Lee, T., W. Hobbs, and J. Willis, et al. (2010), Record warming in the South Pacific and
774 western Antarctica associated with the strong central-Pacific El Niño in 2009-10.
775 *Geophys. Res. Lett.*, 37, L19704, doi:10.1029/2010GL044865
776 Lee, K-W., S.-W. Yeh, J.-S. Kug, and J.-Y. Park, 2014:Ocean chlorophyll response to
777 two types of El Nino events in an ocean-biogeochemical coupled model. J. Geophys.
778 Res., 119, doi:10.1002/2013JC009050.
779 Lengaigne, M., E. Guilyardi, J.P. Boulanger, C. Menkes, P. Delecluse, P. Inness, 2004:
780 Triggering of El Niño by westerly wind events in a coupled general circulation model.
781 Climate Dyn., 23, 601-620.
782 Lübbecke, J., and M.J. McPhaden, 2014:Assessing the Twenty-First-Century shift in
783 ENSO variability in terms of the Bjerknes stability index. J. Climate, 27, 2577-2587.
784 McGregor, S., A. Timmermann, M. H. England, O. Elison Timm, and A. T. Wittenberg,
785 2013: Inferred changes in El Niño-Southern Oscillation variance over the past six
786 centuries. Clim. Past, 9, 2269-2284. doi: 10.5194/cp-9-2269-2013
787 McPhaden, M.J., 1999: Climate oscillations – Genesis and evolution of the 1997-98 El
788 Niño. Science, 283, 950-954.

McPhaden, M.J., 2004: Evolution of the 2002-03 El Niño. Bull. Amer. Meteor. Soc., 85, 677-695.

McPhaden, M. J., T. Lee, and D. McClurg, 2011: El Niño and its relationship to changing background conditions in the tropical Pacific. *Geophys. Res. Lett. 38,* L15709, doi:10.1029/2011GL048275

McPhaden, M.J., 2012: A 21st century shift in the relationship between ENSO SST and Warm Water Volume anomalies. Geophys. Res. Lett., 39, L09706, doi:10.1029/2012GL051826

McPhaden, M.J., and X. Yu, 1999: Equatorial waves and the 1997-98 El Niño. Geophys. Res. Lett., 26, 2961-2964

McPhaden, M.J., S.E. Zebiak, and M.H. Glantz, 2006: ENSO as an intriguing concept in Earth science. Science, 314, 1740-1745.

Meinen, C.S., and M.J. McPhaden, 2000: Observations of warm water volume changes in the equatorial Pacific and their relationship to El Niño and La Niña. J. Climate, 13, 3551-3559.

Moy, C.M., G.O.Seltzer, D.T. Rodbell, and D.M. Anderson, 2002: Variability of El Niño/Southern Oscillation activity at millennial timescales during the Holocene epoch. Nature, 420, 162-165.

National Climatic Data Center (NCDC), 1994: Time bias corrected divisional temperature-precipitation-drought index: Documentation for data set TD-9640, http://www.cdc.noaa.gov/USclimate/Data/, Ashville, NC.

Newman, M., S.-I. Shin, and M. A. Alexander, 2011a: Natural variation in ENSO flavors. *Geophys. Res. Lett*., L14705, doi:10.1029/2011GL047658.

812 Newman, M., M. A. Alexander, and J. D. Scott, 2011b: An empirical model of tropical
813 ocean dynamics. *Climate Dynamics*, **37**, 1823-1841, doi: 10.1007/s00382-011-1034-0
814 Ogata, T., S.-P. Xie, A. Wittenberg, and D.-Z. Sun, 2013: Interdecadal amplitude
815 modulation of El Niño/Southern Oscillation and its impacts on tropical Pacific
816 decadal variability. J. Climate, 26, 7280-7297. doi: 10.1175/JCLI-D-12-00415.1
817 Penland, C., and P.D. Sardeshmukh, 1995: The optimal growthof tropical sea surface
818 temperature anomalies. J. Climate, 8, 1999-2024.
819 Qu, T. and J.-Y. Yu, 2014: ENSO Indices from Sea Surface Salinity Observed by
820 Aquarius and Argo*, Journal of Oceanography*, In Press.
821 Radenac, M.-H., F. Léger, A. Singh, and T. Delcroix, 2012: Sea Surface Chlorophyll
822 signature in the tropical Pacific during eastern and central Pacific ENSO events. J.
823 Geophys. Res., 117, C04007, doi:10.1029/2011JC007841.
824 Rasmusson, E.M., and T.H. Carpenter, 1982: Variations in tropical sea-surface
825 temperature and surface wind fields associated with the Southern-Oscillation El Niño.
826 Mon. Wea. Rev., 110, 354-384.
827 Rayner, N.A., D.E. Parker, E.B. Horton, C.K. Folland, L.V. Alexander, D.P. Rowell, E.C.
828 Kent, and A. Kaplan, 2003: Global analyses of sea surface temperature, sea ice, and
829 night marine air temperature since the late nineteenth century. J. Geophys. Res., 108,
830 10.1029/2002JD002670
831 Rodgers, K. B., P. Friederichs, and M. Latif, 2004: Tropical Pacific decadal variability
832 and its relation to decadal modulations of ENSO. J. Climate, 17, 3761–3774.

833 Ropelewski, C.F., and M.S. Halpert, 1987: Global and regional scale precipitation
834 patterns associated with El Niño/Southern Oscillation. Mon. Wea. Rev., 115, 1606-
835 1626.
836 Sandeep, S., F. Stordal, P.D. Sardeshmukh, and G.P. Compo, 2014: Pacific Walker
837 Circulation variability in coupled and uncoupled climate models. Cli. Dyn., in press,
838 doi:10.1007/s00382-014-2135-3.
839 Schopf, P. S. and R. J. Burgman, 2006: A simple mechanism for ENSO residuals and
840 asymmetry. J. Climate, 19, 3167–3179.
841 Shin, S.-I., P. D. Sardeshmukh, and R. S. Webb, 2010: Optimal tropical sea surface
842 temperature forcing of North American drought. J. Climate, 23, 3907-3917.
843 Shukla, J., and D.A. Paolino, 1983: The Southern Oscillation and long range forecasting
844 of the summer monsoon rainfall over India. Mon. Wea. Rev., 111, 1830-1837.
845 Singh, A., T. Delcroix, and S. Cravatte, 2011: Contrasting the flavors of El Niño and
846 Southern Oscillation using sea surface salinity observations. J. Geophys. Res., 116,
847 C06016, doi: 10.1029/2010JC006862.
848 Solomon, A., and M. Newman, 2012: Reconciling disparate twentieth-century Indo-
849 Pacific ocean temperature trends in the instrumental record. Nature Climate Change,
850 2, 691-699. doi: 10.1038/nclimate1591
851 Smith, T.M., and R.W. Reynolds, 2004: Improved Extended Recontruction of SST
852 (1854-1997). J. Climate, 17, 2466-2477.
853 Stevenson, S., B. Fox-Kemper, M. Jochum, R. Neale, C. Deser, and G. Meehl, 2012: Will
854 there be a significant change to El Niño in the twenty-first century?. J. Climate, 25,
855 2129–2145. doi: 10.1175/JCLI-D-11-00252.1

856 Shin, S.-I., P. Sardeshmukh, and R.S. Webb, 2010: Optimal tropical sea surface
857 temperature forcing of North American drought. J. Climate, 23, 3907-3917
858 Sun, C., M. M. Rienecker, A. Rosati, M. Harrison, A. Wittenberg, C. L. Keppenne, J. P.
859 Jacob, and R. M. Kovach, 2007: Comparison and sensitivity of ODASI ocean
860 analyses in the tropical Pacific. Mon. Wea. Rev., 135, 2242-2264. doi:
861 10.1175/MWR3405.1
862 Sun, F. and J.-Y. Yu: A 10-15year Modulation Cycle of ENSO intensity. *J. Climate*, 22,
863 1718-1735.
864 Takahashi, K., A. Montecinos, K. Goubanova, and B. Dewitte, 2011: ENSO regimes:
865 Reinterpreting the canonical and Modoki El Niño. Geophys. Res. Lett., 38, L10704,
866 doi:10.1029/2011GL047364
867 Taschetto, A., and M.H. England, 2009: El Niño Modoki impacts on Australian rainfall. J.
868 Climate, 22, 3167-3173
869 Tokinaga, H., S.-P. Xie, A. Timmermann, S. McGregor, T. Ogata, H. Kubota, and Y. M.
870 Okumura, 2012a: Regional patterns of tropical Indo-Pacific climate change: Evidence
871 of the Walker circulation weakening. J. Climate, 25, 1689–1710. doi: 10.1175/JCLI-
872 D-11-00263.1
873 Tokinaga, H., S.-P. Xie, C. Deser, Y. Kosaka, and Y. M. Okumura, 2012b: Slowdown of
874 the Walker circulation driven by tropical Indo-Pacific warming. Nature, 491, 439-
875 443. doi: 10.1038/nature11576
876 Trenberth, K.E., G.W. Branstator, D. Karoly, A. Kumar, N.-C. Lau, and C. Ropelewski,
877 1998: Progress during TOGA in understanding and modeling global teleconnections

878 associated with tropical sea surface temperatures. J. Geophys. Res., 103, 14291-
879 14324.
880 Turk, D., C.S. Meinen, D. Antoine, M.J. McPhaden, and M.R. Lewis, 2011: Implications
881 of changing El Niño patterns for biological dynamics in the equatorial Pacific Ocean.
882 Geophys. Res. Lett., 38, L23603, doi:10.1029/2011GL049674.
883 US CLIVAR ENSO Diversity WG, 2013: U.S. CLIVAR ENSO Diversity Workshop
884 Report. Report 2013-1, U.S. CLIVAR Project Office, Washington, DC, 20006, 20pp.
885 Vecchi, G. A., and A. T. Wittenberg, 2010: El Niño and our future climate: Where do we
886 stand? Wiley Interdisciplinary Reviews: Climate Change, 1, 260-270. doi:
887 10.1002/wcc.33
888 Vecchi, G. A., A. T. Wittenberg, and A. Rosati, 2006: Reassessing the role of stochastic
889 forcing in the 1997-8 El Niño. Geophys. Res. Lett., 33, L01706. doi:
890 10.1029/2005GL024738.
891 Vimont, D., M. A. Alexander, and M. Newman 2014: Optimal Growth of Central and
892 East Pacific ENSO Events. Geophys. Res. Lett., in press.
893 Wang, W., and H.H. Hendon, 2007: Sensitivity of Australian rainfall to inter-El Niño
894 variations. J. Climate, 20, 4211-4226.
895 Wang,W., M. Chen, and A. Kumar, 2010:An assessment of the CFS real-time seasonal
896 forecasts. Wea. Forecasting, 25, 950–969
897 Watanabe, M., and A. T. Wittenberg, 2012: A method for disentangling El Niño-mean
898 state interaction. Geophys. Res. Lett., 39, L14702. doi: 10.1029/2012GL052013

899 Watanabe, M., J.-S. Kug, F.-F. Jin, M. Collins, M. Ohba, and A. T. Wittenberg, 2012:
900 Uncertainty in the ENSO amplitude change from the past to the future. Geophys. Res.
901 Lett., 39, L20703. doi: 10.1029/2012GL053305
902 Weng, H., K. Ashok, S.K. Behera, S.A. Rao, and T. Yamagata, 2007: Impacts of recent
903 El Niño Modoki on dry/wet conditions in the Pacific rim during boreal summer.
904 Climate Dyn., 29, 113-129.
905 Wittenberg, A. T., 2004: Extended wind stress analyses for ENSO. J. Climate, 17, 2526-
906 2540. doi: 10.1175/1520-0442(2004)017%3C2526:EWSAFE%3E2.0.CO;2
907 Wittenberg, A. T., A. Rosati, N.-C. Lau, and J. J. Ploshay, 2006: GFDL's CM2 global
908 coupled climate models, Part III: Tropical Pacific climate and ENSO. J. Climate, 19,
909 698-722. doi: 10.1175/JCLI3631.1
910 Wittenberg, A. T., 2009: Are historical records sufficient to constrain ENSO simulations?
911 Geophys. Res. Lett., 36, L12702. doi: 10.1029/2009GL038710
912 Wittenberg, A. T., A. Rosati, T. L. Delworth, G. A. Vecchi, and F. Zeng, 2014: ENSO
913 modulation: Is it decadally predictable? J. Climate, 27, 2667-2681. doi:
914 10.1175/JCLI-D-13-00577.1
915 Xie, S.-P., 1999: A dynamic ocean-atmosphere model of the tropical Atlantic decadal
916 variability. J. Climate, 12, 64-70.
917 Xie, S.-P., C. Deser, G. A. Vecchi, J. Ma, H. Teng, and A. T. Wittenberg, 2010: Global
918 warming pattern formation: Sea surface temperature and rainfall. J. Climate, 23, 966-
919 986. doi: 10.1175/2009JCLI3329.1

920 Xue, Y., M. Chen, A. Kumar, Z.-Z. Hu, W. Wang, 2013: Prediction Skill and Bias of
921 Tropical Pacific Sea Surface Temperatures in the NCEP Climate Forecast System
922 Version 2. J. Climate, 26, 5358-5378
923 Yang, C., and B.S. Giese, 2013: El Niño Southern Oscillation in an ensemble ocean
924 reanalysis and coupled climate models. J. Geophys. Res., Oceans, 118 (9), 4052-4071.
925 Yeh, S.-W., J.-S. Kug, B. Dewitte, M.-H. Kwon, B. Kirtman, and F.-F. Jin, 2009: El Niño
926 in a changing climate. *Nature*. **461**. doi: 10.1038/nature08316
927 Yu., J.-Y. and S. T. Kim, 2010: Identification of Central-Pacific and Eastern-Pacific
928 Types of ENSO in CMIP3 Models*, Geophysical Research Letters*, 37, L15705,
929 doi:10.1029/2010GL044082.
930 Yu, J.-Y., H.-Y. Kao, and T. Lee, 2010: Subtropics-related interannual sea surface
931 temperature variability in the equatorial central Pacific.. J. Climate, 23, 2869-2884.
932 Yu., J.-Y. and S. T. Kim, 2011: Relationships between Extratropical Sea Level Pressure
933 Variations and the Central-Pacific and Eastern-Pacific Types of ENSO*, Journal of*
934 *Climate*, 24, 708-720.
935 Yu, J.-Y., H.-Y. Kao, T. Lee, and S.T. Kim, 2011: Subsurface ocean temperature indices
936 for Central-Pacific and Eastern-Pacific types of El Niño and La Niña events.
937 Theoretical and Applied Climatology, 103, 337-344.
938 Yu., J.-Y., Y. Zou, S. T. Kim, and T. Lee, 2012: The Changing Impact of El Nino on US
939 Winter Temperatures*, Geophysical Research Letters*, doi:10.1029/2012GL052483
940 Yu, J.-Y. and Y. Zou, 2013: The enhanced drying effect of Central-Pacific El Nino on US
941 winter*, Environmental Research Letters*, **8**, doi:10.1088/1748-9326/8/1/014019

942 Yu, J.-Y., and B.S. Giese, 2013: ENSO diversity in observations. U.S. CLIVAR
943 Variations, 11, 1-5.
944 Zavala-Garay, J., C. Zhang, A. M. Moore, A. T. Wittenberg, M. J. Harrison, A. Rosati, J.
945 Vialard, and R. Kleeman, 2008: Sensitivity of hybrid ENSO models to unresolved
946 atmospheric variability. *J. Climate*, **21**, 3704-3721. doi: 10.1175/2007JCLI1188.1.
947 Zebiak, S. E., and M. A. Cane, 1987: A Model El Niño–Southern Oscillation. *Mon. Wea.*
948 *Rev.*, **115**, 2262–2278.
949 Zhang, S., M. J. Harrison, A. Rosati, and A. Wittenberg, 2007: System design and
950 evaluation of coupled ensemble data assimilation for global oceanic climate studies.
951 *Mon. Wea. Rev.*, **135**, 3541-3564. doi: 10.1175/MWR3466.1
952 Zhang, H., A. Clement, and P. Di Nezio, 2014: The South Pacific Meridional Mode: A
953 mechanism for ENSO-like variability. *J. Climate*, 27, 769-783.
954 Zheng, W., Braconnot, P., Guilyardi, E., Merkel, U. and Yu, Y. 2008: ENSO at 6ka and
955 21ka from ocean-atmosphere coupled model simulations. *Climate Dynamics*. **30,** 745-
956 762
957
958
959

960 **Figure captions**

961

962 **Figure 1**. (Left) Distribution of boreal winter (NDJ) SSTA extrema in the longitude-
963 amplitude plane. Anomalies were obtained from the NOAA Extended Reconstructed SST
964 data set (Smith et al. 2004) over the period 1900-2013, as departures from the 1945-2013
965 climatology. Each dot corresponds to the extreme positive or negative value over the NDJ
966 of each year in the region 2°S-2°N, 110°E-90°W. Events prior to 1945 are colored in
967 grey. Events after 1945 are considered EP (red dots) when the Niño3 index exceeds one
968 standard deviation. CP events are identified using the leading principal component of the
969 SSTA residual after removing the SSTA regression onto the Niño3 index. Blue dots in
970 the left panel correspond to events for which the leading principal component (used as CP
971 index) exceeds one standard deviation. The spatial patterns of SSTA for specific warm
972 and cold events of either type are shown on the right panels, with a contour interval of
973 0.25°C.

974

975

976 **Figure 2**. Evolution of SSTAs from the initial conditions shown in the top panels to the
977 final states shown in the middle panels six months later. The initial conditions (i.e.
978 optimal structures) are obtained by determining a linear stochastically forced dynamical
979 model from SSTAs (HadISST data set, Rayner et al. 2003), thermocline depth anomalies
980 (SODA dataset, Carton and Giese 2008) and zonal wind stress anomalies (NCEP
981 Reanalysis, Kalnay et al. 1996), over the period 1959-2000. (a) Evolution of the first
982 pattern (which leads to an EP-type ENSO) shown as maps at (top) t=0, and (middle) t=6

983 months. (b) Same as (a) except for the evolution of the second pattern (which leads to a
984 CP-type ENSO). Anomalous SST is indicated by shading (contour interval 0.25°K),
985 thermocline depth by contours (contour interval 5m, where black is positive), and zonal
986 wind stress by black vectors (scaled by the reference vector 0.02 Nm^{-2}, with values below
987 0.002 Nm^{-2} removed for clarity. Note that in this linear framework, the opposite signed
988 patterns lead to cold events. (Bottom) Projection of observations onto the optimal initial
989 condition for SST anomaly amplification over a six-month interval, vs. the projection on
990 the optimal evolved SST state 6 months later, for (c) the EP pattern, and (d) the CP
991 pattern. Note that the tropical SST growth factor (indicated by the range of the ordinate)
992 for the EP pattern is almost 4 times greater than for the CP pattern. Color shading of dots
993 in the EP (CP) panel indicates the value of the projection on the CP (EP) optimal initial
994 condition. Adapted from Newman et al. (2011a).
995
996 **Figure 3**. Distribution of equatorial Pacific SSTA maxima, for El Niño events occurring
997 in a 4000-year pre-industrial control simulation from the GFDL CM2.1 coupled GCM.
998 To qualify as an El Niño, the simulated DJF-mean SSTA averaged over the Niño3 region
999 (150°W-90°W, 5°S-5°N) must exceed 0.5°C. For each of the 1359 such events, the DJF-
1000 mean SSTA is averaged over the equatorial zone (5°S-5°N), and then the Pacific zonal
1001 maximum is located. (a) Distribution of peak SSTA longitudes (°E). (b) Scatterplot of the
1002 peak SSTA value (°C) versus the longitude (°E) at which it occurs. (c) Distribution of
1003 peak SSTA values (°C).
1004
1005

Figure 4. Composite evolution of zonally-averaged thermocline depth, displayed as a function of latitude and time, for El Niño events occurring in a 500-year pre-industrial control simulation from the NCAR-CCSM4 coupled GCM. The selected events peak in (a) the Niño3 region (150°W-90°W, 5°S-5°N), (b) the Niño4 region (160°E-150°W, 5°S-5°N), and (c) a region displaced 20° to the west of the Niño4 area. The label at the top of each panel indicates the central longitude of the region where each event peaks. January 1 corresponds to the event peak, and the evolution is shown from January of year 0 to the January of year 2. The depth of the 15°C isotherm is used as a proxy for thermocline depth. Adapted from Capotondi (2013).

Figure 5. Composites of U.S. temperature anomalies during autumn (SON) and Winter (DJF) for "Conventional" (i.e. EP) and "Dateline" (i.e. CP) El Niños during 1950-2003. The composites are based on the U.S. Climate Division data set [National Climatic Data Center (NCDC) 1994]. Anomalies are computed relative to the 1950-1995 climatology. The right two columns are masked for 80% statistical significance. From Larkin and Harrison (2005). Courtesy of Drs. N.K. Larkin and D. E. Harrison.

Figure 6. Composites of U.S. precipitation anomalies during autumn (SON) and Winter (DJF) for "Conventional" (i.e. EP) and "Dateline" (i.e. CP) El Niños during 1950-2003. Shown as in Figure 5. From Larkin and Harrison (2005). Courtesy of Drs. N.K. Larkin and D. E. Harrison.

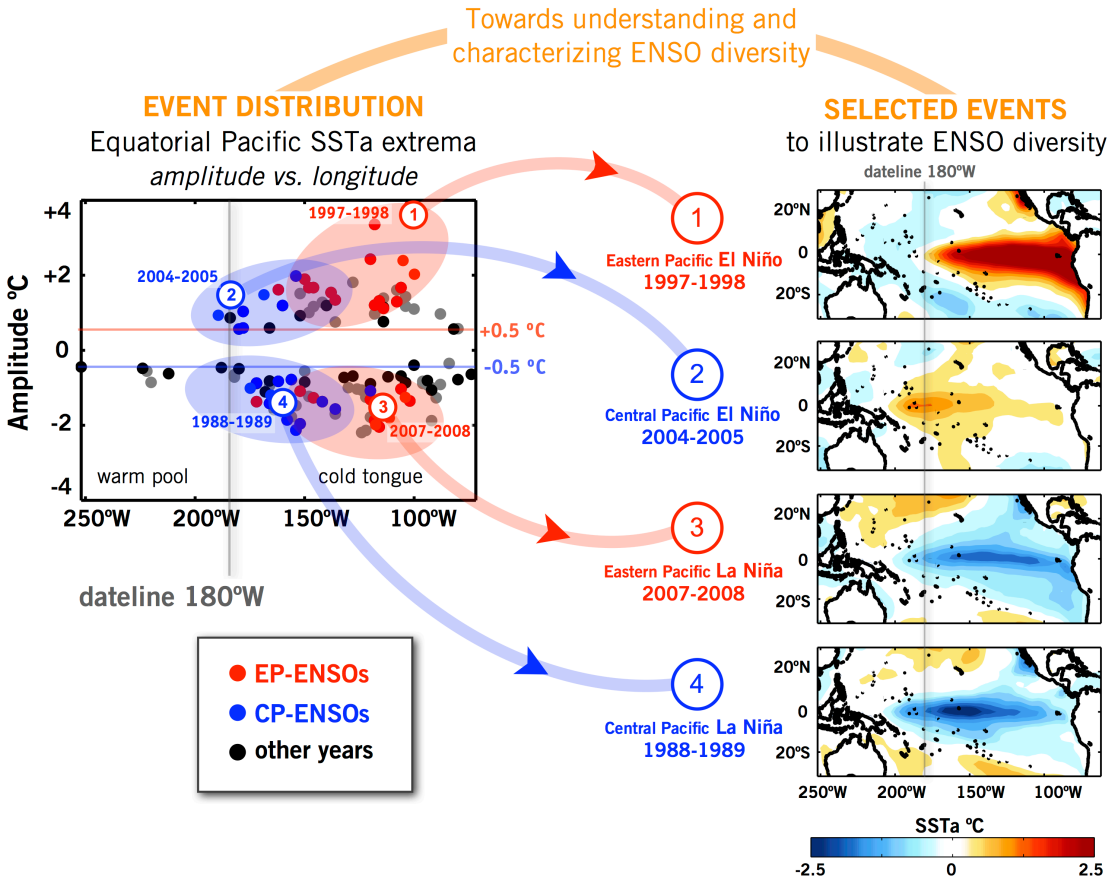

1030
1031

Figure 1. (Left) Distribution of boreal winter (NDJ) SSTA extrema in the longitude-amplitude plane. Anomalies were obtained from the NOAA Extended Reconstructed SST data set (Smith et al. 2004) over the period 1900-2013, as departures from the 1945-2013 climatology. Each dot corresponds to the extreme positive or negative value over the NDJ of each year in the region 2°S-2°N, 110°E-90°W. Events prior to 1945 are colored in grey. Events after 1945 are considered EP (red dots) when the Niño3 index exceeds one standard deviation. CP events are identified using the leading principal component of the SSTA residual after removing the SSTA regression onto the Niño3 index. Blue dots in the left panel correspond to events for which the leading principal component (used as CP index) exceeds one standard deviation. The spatial patterns of SSTA for specific warm and cold events of either type are shown on the right panels, with a contour interval of 0.25°C.

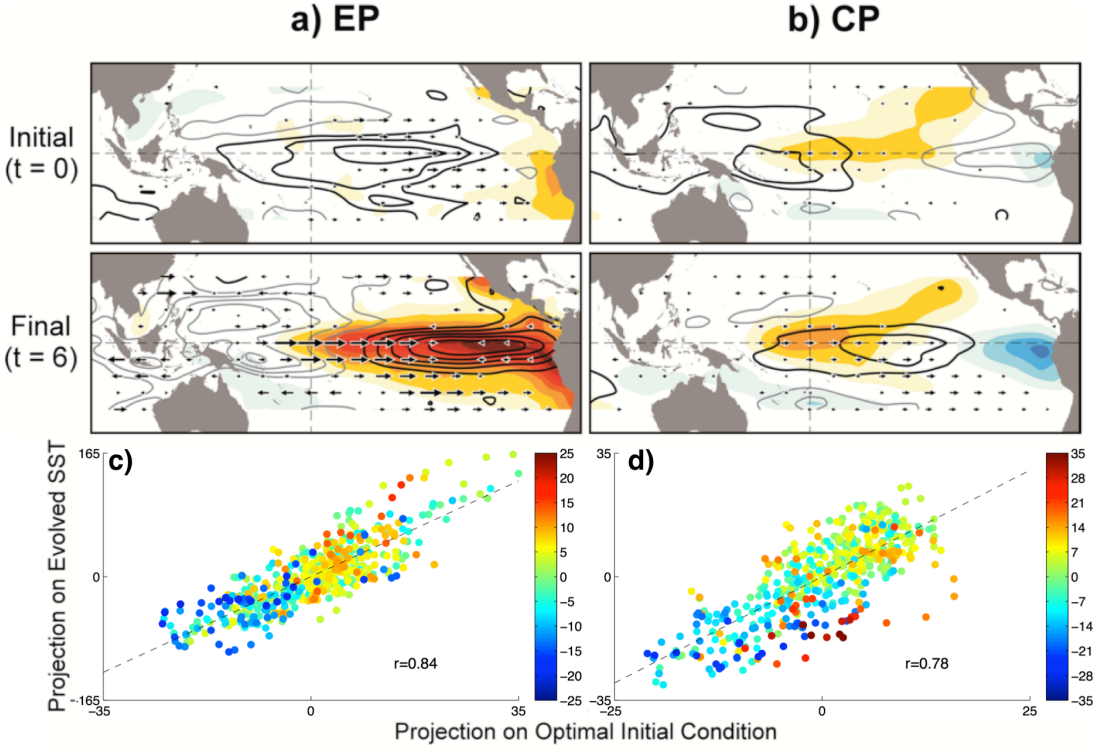

Figure 2. Evolution of SSTAs from the initial conditions shown in the top panels to the final states shown in the middle panels six months later. The initial conditions (i.e. optimal structures) are obtained by determining a linear stochastically forced dynamical model from SSTAs (HadISST data set, Rayner et al. 2003), thermocline depth anomalies (SODA dataset, Carton and Giese 2008) and zonal wind stress anomalies (NCEP Reanalysis, Kalnay et al. 1996), over the period 1959-2000. (a) Evolution of the first pattern (which leads to an EP-type ENSO) shown as maps at (top) t=0, and (middle) t=6 months. (b) Same as (a) except for the evolution of the second pattern (which leads to a CP-type ENSO). Anomalous SST is indicated by shading (contour interval 0.25°K), thermocline depth by contours (contour interval 5m, where black is positive), and zonal wind stress by black vectors (scaled by the reference vector 0.02 Nm^{-2}, with values below 0.002 Nm^{-2} removed for clarity. Note that in this linear framework, the opposite signed patterns lead to cold events. (Bottom) Projection of observations onto the optimal initial condition for SST anomaly amplification over a six-month interval, vs. the projection on the optimal evolved SST state 6 months later, for (c) the EP pattern, and (d) the CP pattern. Note that the tropical SST growth factor (indicated by the range of the ordinate) for the EP pattern is almost 4 times greater than for the CP pattern. Color shading of dots in the EP (CP) panel indicates the value of the projection on the CP (EP) optimal initial condition. Adapted from Newman et al. (2011a).

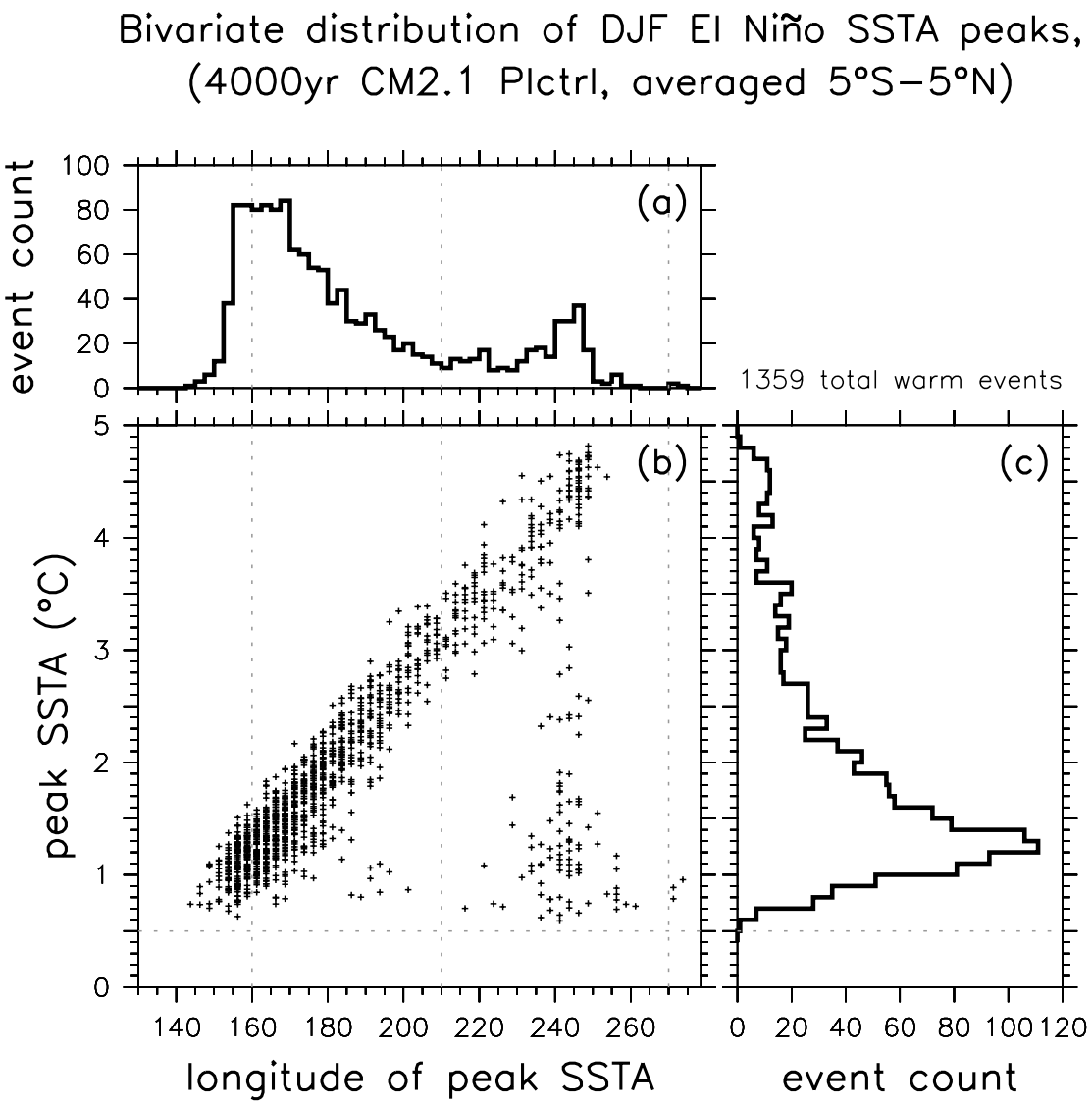

Figure 3. Distribution of equatorial Pacific SSTA maxima, for El Niño events occurring in a 4000-year pre-industrial control simulation from the GFDL CM2.1 coupled GCM. To qualify as an El Niño, the simulated DJF-mean SSTA averaged over the Niño3 region (150°W-90°W, 5°S-5°N) must exceed 0.5°C. For each of the 1359 such events, the DJF-mean SSTA is averaged over the equatorial zone (5°S-5°N), and then the Pacific zonal maximum is located. (a) Distribution of peak SSTA longitudes (°E). (b) Scatterplot of the peak SSTA value (°C) versus the longitude (°E) at which it occurs. (c) Distribution of peak SSTA values (°C).

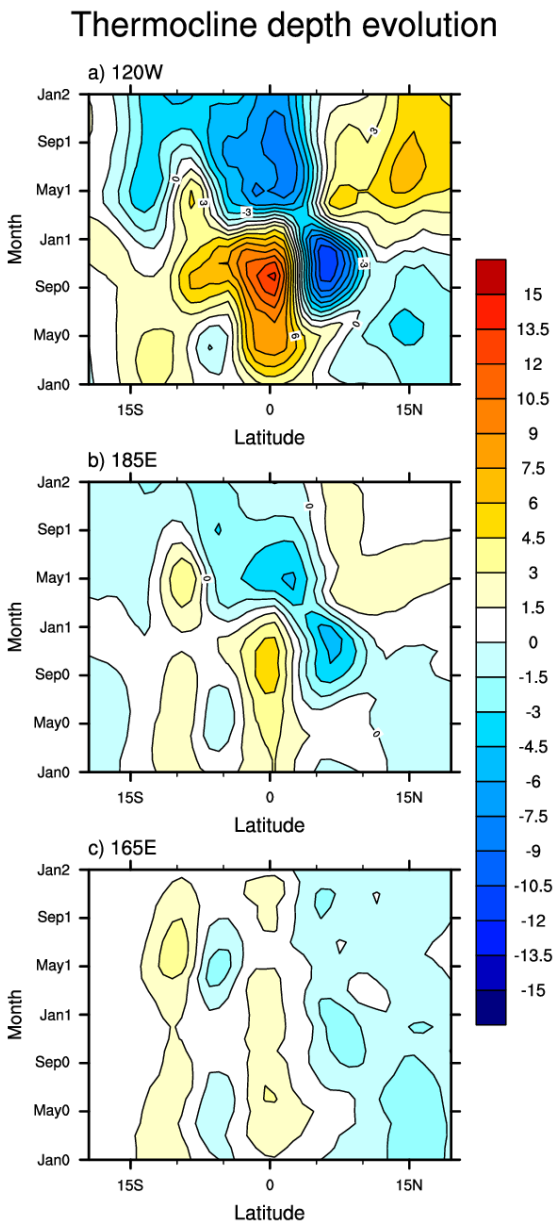

1039
1040

Figure 4. Composite evolution of zonally-averaged thermocline depth, displayed as a function of latitude and time, for El Niño events occurring in a 500-year pre-industrial control simulation from the NCAR-CCSM4 coupled GCM. The selected events peak in (a) the Niño3 region (150°W-90°W, 5°S-5°N), (b) the Niño4 region (160°E-150°W, 5°S-5°N), and (c) a region displaced 20° to the west of the Niño4 area. The label at the top of each panel indicates the central longitude of the region where each event peaks. January 1 corresponds to the event peak, and the evolution is shown from January of year 0 to the January of year 2. The depth of the 15°C isotherm is used as a proxy for thermocline depth. Adapted from Capotondi (2013).

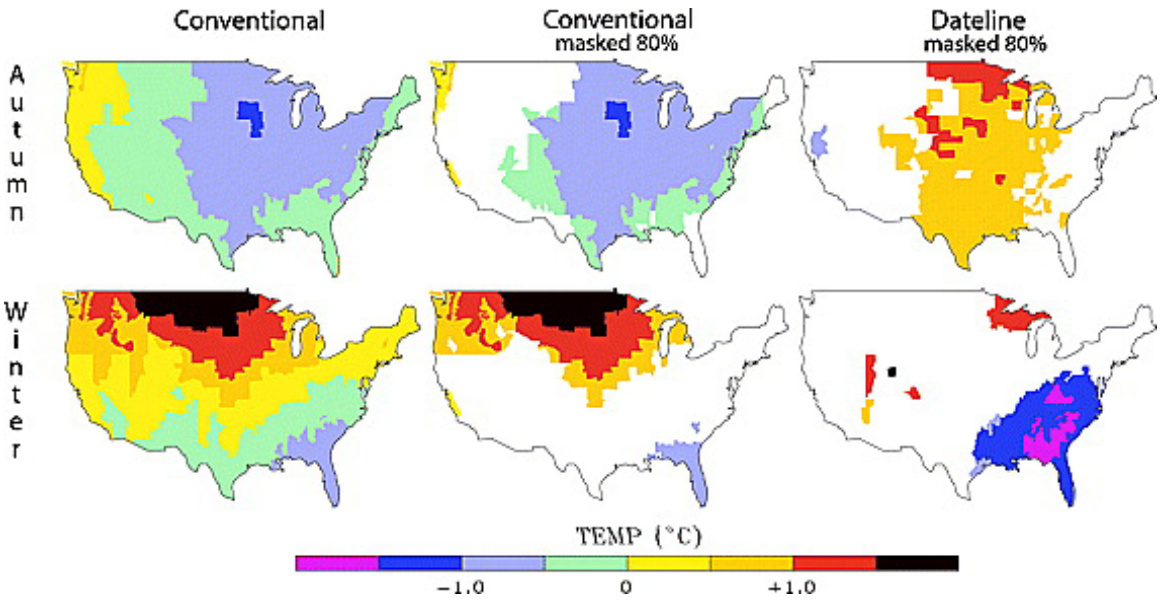

1041

Figure 5. Composites of U.S. temperature anomalies during autumn (SON) and Winter (DJF) for "Conventional" (i.e. EP) and "Dateline" (i.e. CP) El Niños during 1950-2003. The composites are based on the U.S. Climate Division data set [National Climatic Data Center (NCDC) 1994]. Anomalies are computed relative to the 1950-1995 climatology. The right two columns are masked for 80% statistical significance. From Larkin and Harrison (2005). Courtesy of Drs. N.K. Larkin and D. E. Harrison.

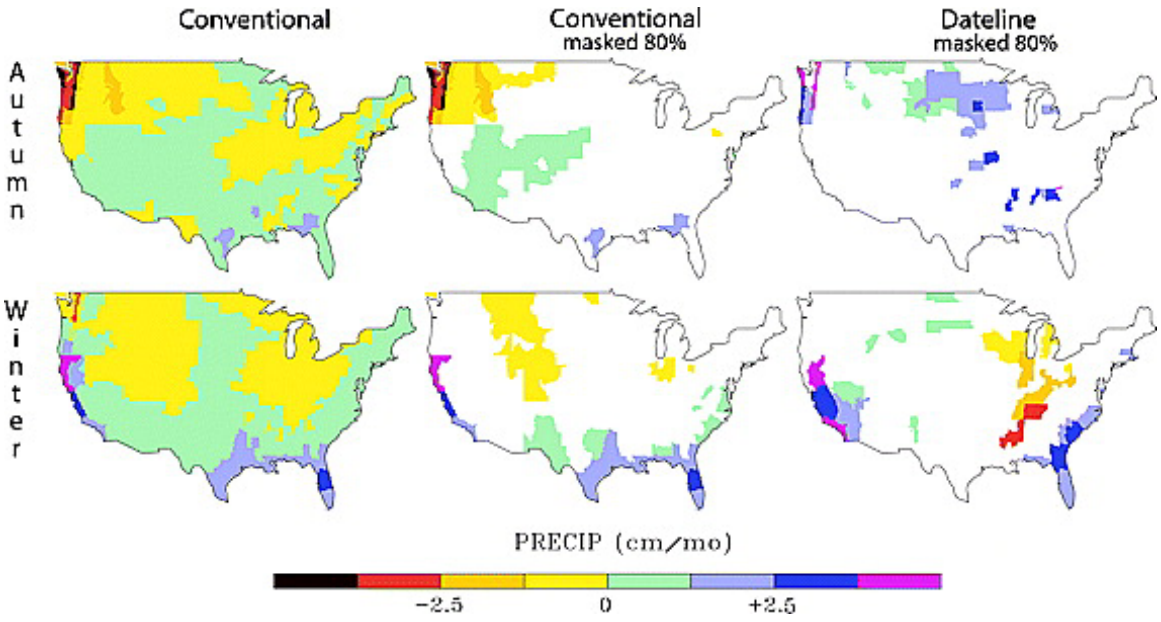

Figure 6. Composites of U.S. precipitation anomalies during autumn (SON) and Winter (DJF) for "Conventional" (i.e. EP) and "Dateline" (i.e. CP) El Niños during 1950-2003. Shown as in Figure 5. From Larkin and Harrison (2005). Courtesy of Drs. N.K. Larkin and D. E. Harrison.